

Control of Stability and Structure of Liposomes by Means of Nanoparticles

Raphaël Michel, Tobias Plostica, Ludmila Abezgauz, Dganit Danino, Michael Gradzielski

▶ **To cite this version:**

Raphaël Michel, Tobias Plostica, Ludmila Abezgauz, Dganit Danino, Michael Gradzielski. Control of Stability and Structure of Liposomes by Means of Nanoparticles. Soft Matter, 2013, 9 (16), pp.4167. 10.1039/C3SM27875A . hal-03723877

HAL Id: hal-03723877
https://hal.science/hal-03723877

Submitted on 6 Oct 2022

HAL is a multi-disciplinary open access archive for the deposit and dissemination of scientific research documents, whether they are published or not. The documents may come from teaching and research institutions in France or abroad, or from public or private research centers.

L'archive ouverte pluridisciplinaire **HAL**, est destinée au dépôt et à la diffusion de documents scientifiques de niveau recherche, publiés ou non, émanant des établissements d'enseignement et de recherche français ou étrangers, des laboratoires publics ou privés.

Control of Stability and Structure of Liposomes by Means of Nanoparticles

Raphael Michel[a], Tobias Plostica[a], Ludmila Abezgauz[b], Dganit Danino[b] and Michael Gradzielski[a]

Received (in XXX, XXX) Xth XXXXXXXXX 20XX, Accepted Xth XXXXXXXXX 20XX
DOI: 10.1039/b000000x

The interaction of bilayer vesicles with hard nanoparticles is of great relevance to the field of nanotechnology, e.g., its impact on health and safety matters, and also as vesicles are important as delivery vehicles. In this work we describe hybrid systems composed of zwitterionic phospholipid vesicles (DPPC), which are below the phase transition temperature, and added silica nanoparticles (SiNPs) of much smaller size. The initial DPPC unilamellar vesicles, obtained by extrusion, are rather unstable and age but the rate of ageing can be controlled over a large time range by the amount of added SiNPs. For low addition they become destabilized whereas larger amounts of SiNPs enhance the stability largely as confirmed by dynamic light scattering (DLS). ζ-potential and DSC measurements confirm a binding of the SiNPs onto the phospholipid vesicles, which stabilizes the vesicles against flocculation by rendering the ζ-potential more negative. This effect appears above a specific SiNP concentration, and is the result of the adsorption of the negatively charged nanoparticles onto the outer surface of the liposome leading to decorated vesicles as proven by cryogenic transmission electron microscopy (cryo-TEM). Small amounts of surface-adsorbed SiNPs initially lead to a bridging of vesicles thereby enhancing flocculation while higher amounts render the vesicles much more negatively charged and thereby long-time stable. This stability has an optimum at neutral pH and for low ionic strength. Thus we show that the addition of the SiNPs is a versatile way to control the stability of gel-state phospholipid vesicles and also to modulate their surface structure in a systematic fashion. This is not only of importance for understanding the fundamental interaction between SiNPs and bilayer vesicles, but also with respect to using silica particles as formulation aids for phospholipid dispersions.

Introduction

Phospholipids are amphiphilic molecules composed of a hydrophilic headgroup (phosphate) and two hydrocarbon chains granting them a truncated cone geometry.[1] Thus phospholipids typically have a tendency for the formation of bilayers, either planar or in the form of closed bilayers, i.e., vesicles.[2, 3]
Being rather versatile self-assembled systems with respect to size and detailed structure, vesicles, which for the case of phospholipids are often called liposomes, are frequently employed in pharmaceutical[4, 5] and cosmetic formulations or for drug delivery.[6-8] This is the case as they are able to transport hydrophobic molecules within their bilayer and/or hydrophilic molecules in their interior, thereby being very flexible carrier systems. Even more importantly, phospholipids are the main component of natural membranes and thereby their vesicle bilayers can serve as good model systems to study interactions of particles or other colloidal systems with biological membranes.

Typically vesicle formation occurs only after an appropriate preparation such as applying ultrasound, rehydration of a lipid film, or extrusion.[9] This is required as normally the equilibrium state of phospholipids is a lamellar phase, whereas vesicles are only metastable.[10] However, that also imposes one of the main limitations of applications of phospholipid vesicles as they are intrinsically unstable[10] and often have a tendency to flocculate.[11, 12] This applies in particular to the case of gel vesicles where bilayer undulations are reduced by the high rigidity of the membrane.[13] Accordingly, comprehensive work has been devoted to their stabilisation against precipitation or flocculation. A classical way of stabilizing vesicles consists in incorporating PEG-ylated lipids into the membrane which leads to steric stabilisation.[14-19] Similarly the adsorption of polyelectrolyte (chitosan and hyaluronan) has been found to stabilize vesicles against pH, osmotic and salt shocks.[20-22]

More recently, novel strategies involving charged nanoparticles have been proposed in order to achieve the stabilisation of liposomes.[23-25] The adsorption of such nanoparticles on vesicle membranes, forming decorated vesicle structures, is believed to allow for the stabilisation of the vesicle dispersion by introducing repulsive electrostatic interactions between the vesicle/nanoparticle complexes. However, considering the potential cytotoxicity of nanoparticles[26] and their various ways of interacting with lipid membrane,[27] further fundamental studies are necessary on this mixed system in order to gain a systematic understanding of this effect of vesicle stabilisation, which will depend on the details of the interaction between nanoparticles and vesicle membrane, as well as on the nature of the phospholipid membrane.

Therefore such a system was studied with a systematic variation of the amounts of added nanoparticles. This was done with the idea of gaining an insight into the detailed control of stability and find optimum conditions for stabilisation, as it is relevant for potential future applications.

Accordingly, we studied the interaction between zwitterionic unilamellar phospholipid vesicles obtained by extrusion and small silica nanoparticles (SiNPs) in water by visual inspection, dynamic light scattering (DLS), ζ-potential measurements, and

cryo-transmission electron microscopy (cryo-TEM). It might be noted that for our investigations we choose DPPC (dipalmitoylphosphatidylcholine) which at 25 °C is well below its phase transition temperature of 41 °C, i.e., the chains are in the crystalline state and the individual molecules in the aggregates are accordingly frozen. Therefore these vesicles are dispersions of vesicles in the gel state, as they are often employed in liposome applications.[5, 8, 28] In order to gain a thorough insight into the interaction with the SiNPs their concentration was varied over a large range.

The obtained results shed light on the effect of vesicle stabilisation upon SiNP addition, thereby allowing to exploit this phenomenon in a systematic way, which is important for formulation purposes. Such knowledge is not only interesting from a fundamental point of view but also for its relevant implications for the use of nanoparticles in imaging or drug delivery. Furthermore the interaction of nanoparticles with lipid membranes is one key aspect in understanding potential toxicity effects of such nanoparticles on cells ("nanotoxicity"), for which liposomes may serve as a good model system.

Materials & Methods

Materials.

1,2-dipalmitoyl-*sn*-glycero-3-phosphocholine (DPPC, 16:0 PC, 99.0%) was obtained from NOF Corporation (Tokyo, Japan) and was used without further purification. Its main phase transition temperature is 41°C.[29-31] The absence of impurities in the lipid bilayer and the formation of the different phases (gel phase, ripple phase and liquid phase) were checked by differential scanning calorimetry (DSC) measurements (see DSC section) performed with a MC-DSC System (TA Instrument, New Castle, DE, USA).

Ludox® HS 40 (colloidal silica suspension, 40 wt.% in water), was purchased from Sigma Aldrich. The particle radius was measured by small angle X-ray scattering (SAXS), performed with a SAXsess apparatus, Anton Paar, (see Fig. S1 in ESI) and found to be 8.36 nm.

Sodium chloride (NaCl, 99.5%) and sodium hydroxide (NaOH, 98%) were purchased from Carl Roth GmbH. Sodium phosphate dibasic dihydrate ($Na_2HPO_4.2H_2O$, 99.5%) and potassium phosphate monobasic (KH_2PO_4, 99.5%) were purchased from sigma Aldrich. Potassium chloride (KCl, 99.5%) was purchased from Merck and hydrochloric acid (HCl, 35-38% in water) from Th. Geyer GmbH.

Sample Preparation.

Unilamellar vesicles (ULVs) of well-defined size were prepared from aqueous lipid mixtures by extrusion through polycarbonate membranes (Whatman®; nominal pore diameters of 200 and 100 nm) by means of a LIPEX™ 10 ml Thermobarrel Extruder. The vesicles were extruded at a temperature above the phase transition temperature, at which the vesicles are in their liquid phase. The extrusion was repeated at least 10 times with both types of membranes subsequently (first 200 then 100 nm pores) to obtain a suspension of quite monodisperse unilamellar vesicles (PDI < 0.1 measured by DLS) of hydrodynamic radius in the range from around 45 nm.

The colloidal suspension of silica nanoparticles was dialysed for two days in water using VISKING® dialysis tubes (ROTH, Karlsruhe, Germany), renewing the dialysis water at least 5 times during this period.

Once obtained, the extruded vesicle solution and the dialyzed nanoparticle solution at the chosen concentration were slowly mixed together under stirring at 65 ± 5°C, i.e., far above the phase transition temperature of DPPC. The mixtures were then stored above the phase transition temperature for 5 minutes and finally allowed to cool down to room temperature (22 ± 2°C) for about 30 minutes before being used for characterization. In the hereby presented series of samples the phospholipid concentration is kept constant and equal to 0.1 wt.%, while the nanoparticle concentration is varied from 0 to 0.15 wt.%. No additional buffer was added to control the pH of these samples (as we wanted to work at low ionic strength) yielding pH values dependent on the particle concentration and thus varying from 7 (in the case of the pure vesicles) to 8.8 (in the case of [NP]/[Vesicle] = 27.7).

The samples at pH 6 and 10 were prepared by adding the appropriate amounts of HCl or NaOH to the silica and phospholipid dispersions. In addition, we prepared for a comparison samples in PBS buffer (137mM NaCl, 2.7 mM KCl, 10mM Na_2HPO_4 and 2mM KH_2PO_4 in Milli-Q water), to see the effect of enhanced ionic strength and to be close to physiological conditions. Otherwise the samples were prepared and treated as described above.

Methods.

Dynamic Light Scattering (DLS). The Dynamic Light Scattering measurements were made using an ALV/CGS-3 Compact Gogniometer system with an ALV/LSE-5004 multiple tau digital correlator (ALV, Langen, Germany), using a 90° scattering geometry and a 632 nm diode laser. All experiments were done in a thermostated bath at 25±0.1°C.

Differential Scanning Calorimetry (DSC). Phase transition temperatures and transition enthalpies were obtained using a TA instruments (New Castle, DE, USA) Multi-Cell Differential Scanning Calorimeter (MC-DSC). After preparation, samples were degassed at room temperature under vacuum in a TA instruments degassing station for about 30 minutes. The measurements were then performed using a scan rate of 0.15°C/min from 15 to 60°C and respecting an equilibration time of 600 seconds prior to each scan.

ζ-Potential Measurements. ζ-Potential measurements were performed at 25°C on a Zeta Sizer-Nano series (Malvern Instruments, Worcestershire, UK) using the Smoluchowski model for the calculation of the ζ-Potential from the measured electrophoretic mobility. The pH values were adjusted by adding small amounts of diluted NaOH and HCl solutions to the samples.

Cryogenic-Transmission Electron Microscopy (cryo-TEM). The samples were prepared on Quantifoil carbon-coated copper grids with a 200 mesh. Samples were prepared in a Vitrobot (FEI) at controlled temperature (25 °C) and humidity (100%

humidity). A grid held by tweezers was dipped into a vial containing the sample. The tweezers were then pneumatically lifted from the sample to an area between two blotting papers where the grid was blotted automatically with specified time of blotting and number of blots (typically 1 blot of 1 second). After a given relaxation time (typically 30 seconds), the grid was rapidly plunged in liquid ethane and vitrified. The sample was then studied in an FEI Tecnai G2 12 Twin transmission electron microscope at a voltage of 120kV. The sample was kept at -175 °C or lower with a Gatan 626 cryo-specimen holder. Images were digitally recorded[32, 33] with a Gatan UltraScan 1000 CCD camera at about 3 micrometers of underfocus.

Volume and Surface Calculation. The calculation of the concentration ratio between particle and liposome was carried out as follows:

The number of vesicles N_V was calculated from the ratio between the number of phospholipid molecules in the bulk N'_{bulk} and the number of phospholipid molecules in one vesicle N'_{ves}:

$$N_V = \frac{N'_{Bulk}}{N'_{Ves}} \quad (1)$$

where N'_{bulk} is given by the mass of lipid added to the system divided by its molecular weight and N'_{Ves} was obtained from the volume of a single vesicle V_{ves} divided by the volume occupied by one lipid molecule within the vesicle membrane V_{lip}. V_{ves} was calculated using the following equation:

$$V_{ves} = \frac{4\pi}{3}(R_{ext}{}^3 - R_{\text{int}}{}^3) \quad (2)$$

The value of the outer radius of the vesicle R_{ext} was taken from the hydrodynamic radius value obtained by DLS measurements at 25°C and assumed to be equal to 42 nm, while the inner radius R_{int} is given by:

$$R_{\text{int}} = R_{ext} - d \quad (3)$$

d being the thickness of the membrane below its phase transition temperature (see Table 1.).[34] It is to be noted that the value of d is this of a steric bilayer thickness as defined in reference 32, i.e., containing n_w water molecules per phospholipid molecule.[34]

The volume of a single lipid V_{lip} within the bilayer is given by the equation:

$$V_{lip} = V_0 + n_w V_w \quad (4)$$

where V_0 is the volume of the dry lipid, n_w the number of water molecules bound to the phospholipid headgroup and V_w the volume of one water molecule (see Table 1.).

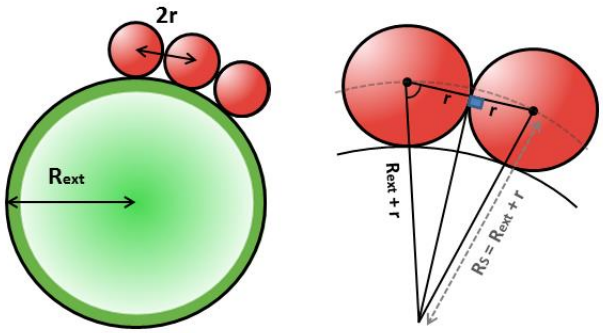


Fig. 1: Schematic drawing of nanoparticles (red spheres) adsorbed on a curved surface (not to scale).

The number of nanoparticles in the system N_{NP} was calculated from the ratio between the mass of the silica introduced in the solution m_{sil} and the mass of a single nanoparticle m_{NP}.

$$N_{NP} = \frac{m_{sil}}{m_{NP}} \quad (5)$$

where m_{NP} is given by the volume of one silica nanoparticle V_{NP} multiplied by its density (taken equal to that of vitreous silica (2.20 g.cm^{-3}), as successfully used in recent neutron scattering contrast variation experiments).[35] V_{NP} was calculated as the volume of a sphere of radius 8.36 nm (mean radius of the nanoparticles measured by SAXS).

Table 1: Parameters used for the calculation of the volume and surface of DPPC vesicles in their gel phase (20°C): the volume of the dry lipid, V_0, the number of water molecules bound to the head group, n_w, the volume of one water molecule, V_w, and the thickness of the bilayer, d. information reprinted with permission from reference 34.[34]

V_0 (Å^3)	n_w	V_w (Å^3)	d (Å)
1144	3.7	30	52.44

Maximum surface coverage calculation: Assuming that SiNPs are systematically adsorbing on the outer surface of the liposomes, the percentage of the liposome surface covered with nanoparticles was determined as follows.

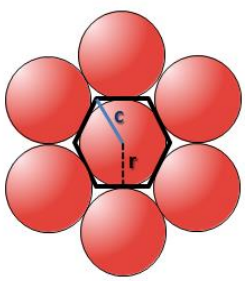


Fig. 2: Schematic drawing of hexagonally packed nanoparticles.

The maximum coverage is obtained when the SiNPs are closely packed: touching each other and with a distance of twice their radius between their centre (Figure 1).

Looking at Figure 1 and taking into account the size difference between nanoparticle and vesicle which allows for considering the vesicle surface as a flat surface, it appears clear that to a very good approximation calculating the coverage of small spheres of

radius r on a curved vesicle surface corresponds to placing the small spheres on a flat surface of total area A_S of a sphere with radius $R_S = R_{ext} + r$.

At this point, the number of SiNP (N_C) needed to achieve the total coverage of the vesicle surface is given by the ratio of the surface A_S with the surface of the hexagon that defines the area occupied by one silica sphere of radius r on the membrane (A_h) (Figure 2.). Hence, N_C can be written:

$$N_C = \frac{A_S}{A_h} \tag{6}$$

where A_S is the surface of a sphere of radius R_S and A_h is calculated from r of a silica sphere adsorbed on the flat surface (see Figure 2) and the length of the hexagon vertice c as follows:

$$A_h = 3\frac{cr}{2} = \frac{6r^2}{\sqrt{3}} \tag{7}$$

Taking 8.36 nm for the radius r of the SiNP (r from SAXS) and 42 nm for the vesicle radius R_{ext} (from DLS) the total surface coverage would be obtained when approximately 132 SiNPs are adsorbed on one vesicle.

Using the calculation presented above, the concentration ratios and the percentage of the surface coverage were calculated for our different experimental SiNP concentrations and listed in table 2.

Table 2: Values of the calculated concentration ratio [NP]/[Vesicle] and surface coverage for different SiNP concentrations, the phospholipid (DPPC) concentration is kept constant and equal to 0.1 wt.%.

SiNP Concentration (wt.%)	*[NP]/[Vesicle]*	*Surface Coverage (%)*
0.025	4.6	3.5
0.0375	6.9	5.3
0.05	9.2	7.0
0.07	12.9	9.8
0.085	15.7	11.9
0.1	18.5	14.0
0.15	27.7	21.0
0.225	41.6	31.7

Results

Stability

Visual Inspection. As a first step we characterized the phase behaviour of mixtures containing extruded phospholipid vesicles and silica nanoparticles as a function of time in order to get insight into the stability of such dispersions and the ageing processes taking place. This was done by regular visual inspection of samples with a constant DPPC vesicle concentration (0.1 wt.% ; 1.36 mM) and different Ludox nanoparticle concentrations (from 0 to 0.15 wt.% - see Fig. 3 and table 2). These samples were stored at room temperature (22 ± 2°C: far below the chain melting temperature of DPPC) for the whole study period.

A first interesting observation is the apparent stabilisation of the vesicle system upon the addition of rather large amounts of silica nanoparticles (see samples containing [NP]/[Vesicle] > 12 in Fig. 3). This is rather surprising, considering that at room temperature, the gel phase vesicles are known to be unstable and to precipitate within some days. This instability is due to the immobility of the lipid molecules and their bilayer. Accordingly in such bilayer systems the repulsive undulation forces are lacking which often are the main contribution to the stability of vesicle dispersions. For these gel-state vesicles the attractive van der Waals interactions dominate, thereby leading to flocculation and subsequent phase separation.

The samples stabilized with sufficiently high content of nanoparticles remain stable for months, despite being well below the main phase transition temperature. For those samples, phase separation occurs only after a time period varying from a few months to more than a year. This is an enormous enhancement compared to the case of pure DPPC vesicles, where precipitation takes place within a few days (see sample [NP]/[Vesicle] = 0 in Fig. 3).

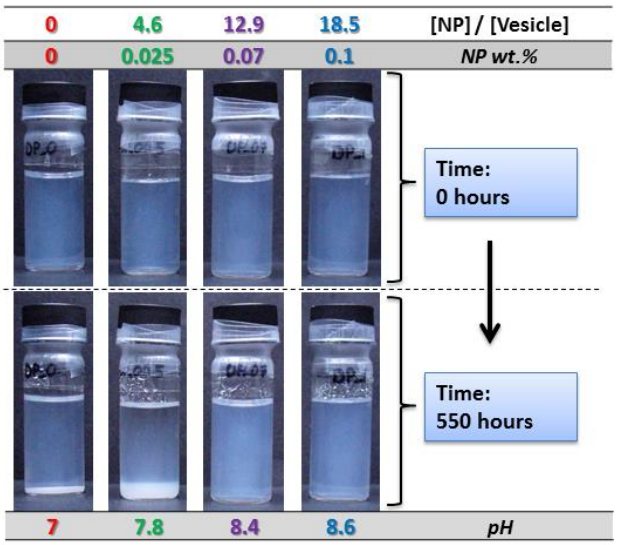


Fig. 3: Photographs of samples containing different ratio [NP]/[Vesicle] shortly after preparation and 550 hours after preparation.

However, this stabilisation effect is only achieved beyond a certain minimum amount of SiNP. The addition of smaller amounts does the contrary; it accelerates the sample destabilisation as shown by the phase separation in Fig. 3 for [NP]/[Vesicle] = 4.6. This effect, as it has been observed in similar systems,[25, 36] is believed to be the result of the presence of negatively charged nanoparticles which will attract neighbouring liposomes, bridging them together thereby accelerating their fusion or aggregation.

Dynamic Light Scattering (DLS). In order to get a more detailed and quantitative understanding of this stabilisation effect, we followed the evolution of the mean particle size in these samples by DLS.

The hydrodynamic radius values were obtained by analysing the scattering intensity correlation functions with a cumulant fit (see ESI).[37] Taking into account the size asymmetry in our system (small nanoparticles, large vesicles) and the resulting difference in scattering intensity, this analysis only allows for the observation of the larger colloids or aggregates in the mixed systems. However, this is exactly what we want to observe as it

reacts rather sensitively to the formation of agglomerates, which is the first step towards flocculation and phase separation.

In the case of the pure DPPC solution, the liposomes in their gel phase fuse or aggregate leading to an increase of their average size (Fig. 4) and a global destabilisation of the vesicle dispersion occurring within a time period varying from a few days to a few weeks.

In the case of the samples with low SiNP concentrations and in agreement with the observations made by visual inspection, the instability occurs earlier as shown by the dramatic increase of the mean hydrodynamic radius at the beginning of the storage time (Fig. 4; sample with [NP]/[vesicle] = 4.6). In the cases mentioned above (pure vesicle solution and samples with low amounts of SiNP) it is basically impossible to precisely predict the time during which the samples remain stable before precipitating since the destabilisation is driven by nucleation processes over which the experimentalist has little influence. It might be noted that the formation of agglomerates is evidenced by DLS not only by the increasing average hydrodynamic radius but also by a concomitant increase of the polydispersity (Fig. S2 - ESI) as now vesicle agglomerates (dimers, trimers, etc. glued together by the SiNPs) are contained.

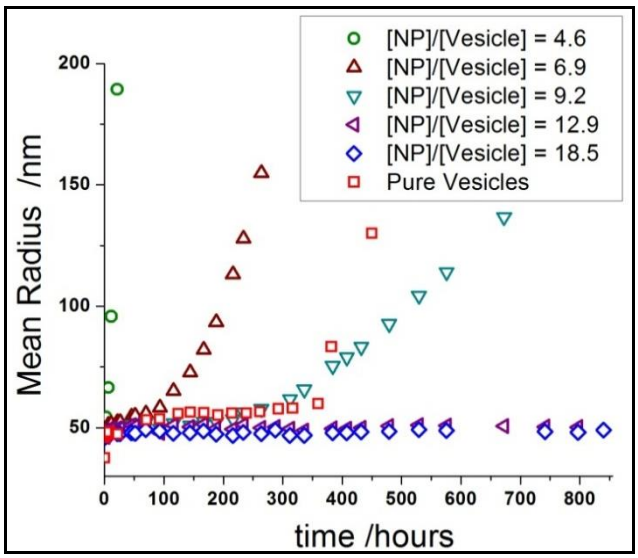


Fig. 4: Temporal evolution of the hydrodynamic radius obtained by DLS in samples containing different ratio [NP]/[Vesicle].

However, when adding more SiNPs we gain control over the chronological order in which the samples get unstable, since the rate of destabilisation now depends systematically on the SiNP concentration. In the case of more concentrated samples ([NP]/[Vesicle] > 12), the higher stability observed by visual inspection and DLS is related to the conservation of the average hydrodynamic radius. For these samples the hydrodynamic radius of the colloidal structures stays around 45-50 nm for more than a month. In this case and assuming that the number of added particles is proportional to the amount of particles finally adsorbed on the vesicle surface, one can argue that a limit in adsorbed silica has been reached, corresponding to a sufficient coverage of the liposomes to ensure the repulsion between the nanoparticle/liposome complexes. Thus, the so-formed decorated vesicles remain stable due to the repulsive electrostatic interactions between their adsorbed particles (see Figs. 5 and 7).

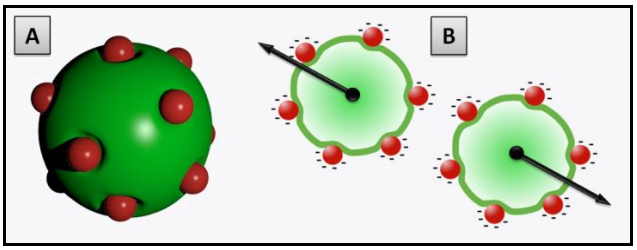


Fig. 5: Schematic drawing of a decorated vesicle structure featuring the local membrane bending caused by the particle adsorption (to scale) (A). Electrostatic repulsion (arrows) between the adsorbed charged nanoparticles responsible for the colloidal stabilisation of the liposome dispersion (B). Figure reprinted with permission from reference 27. [27]

Differential Scanning Calorimetry (DSC). Assuming that the adsorption of nanoparticles on the liposome surface is responsible for the observations made with DLS, it is of central interest to gain further insight into the influence of particle adsorption on the structure of the lipid membrane.

This has been done by differential scanning calorimetry, observing the evolution of the transition temperature and the transition enthalpy in mixed systems with increasing particle concentration. This method should allow to detect local changes of the membrane structure as they would be reflected in the calorimetric transitions. The resulting thermograms and corresponding transition enthalpies as a function of the amount of added SiNPs are presented in Figure 6.

Firstly, the adsorption of increasing amounts of particles has only a very small effect on the membrane transition temperature as the temperature at the peak maximum decreases only somewhat from around 42.05°C (for the pure vesicle solution, in good agreement with values found in the literature for DPPC membranes)[30, 38, 39] to 41.85°C for the more concentrated mixed system. Hence the adsorption of particles does not significantly alter the integrity of the vesicle membrane. However, a widening of the transition region is observed with increasing nanoparticle concentration. These last results can be correlated with those obtained in the case of membranes adsorbed on curved surfaces, where increasing curvature has been found to induce a decrease in the transition temperature coming along with a widening of the transition peak,[38] thereby suggesting that in our system, the particle adsorption leads to local bending of the membrane at the particle location (as depicted in Figure 5.).

In contrast to the transition temperature, the transition enthalpy decreases substantially with increasing nanoparticle concentration (see Figure 6-B). This is to be related with the work of Wang et al.[40] which reveals that the presence of negatively charged nanoparticles on PC membrane induces lipid ordering in the vicinity of the adsorbed particles, i.e., local gelation or ordering in an otherwise fluid membrane. Hence, the creation of such restructured patches would lead to a pronounced decrease of the quantity of lipid membrane taking part in the phase transition, thereby lowering the transition enthalpy. However, the measured transition enthalpy does not decrease linearly with the amount of added particles as seen in Figure 6-B. On the contrary, it seems to reach a plateau when the concentration [NP]/[Vesicles] exceeds 15. Here the enthalpy is reduced by more than 20% showing that a substantial part of the alkyl chains of the DPPC is affected by

the adsorption of the SiNPs. The occurrence of a plateau for [NP]/[Vesicles] > 15 could mean that further added SiNPs do not bind to the vesicle surface but could also be explained by the fact that an adsorbed particle induces structural reconstruction of the membrane on a surface area larger than the one it occupies directly. Thus, above a specific NP concentration, additional particles adsorb on membrane areas already affected by the presence of neighbouring particles, such that these additional particles have less or no effect on the membrane structure, thereby having a reduced influence on the transition enthalpy.

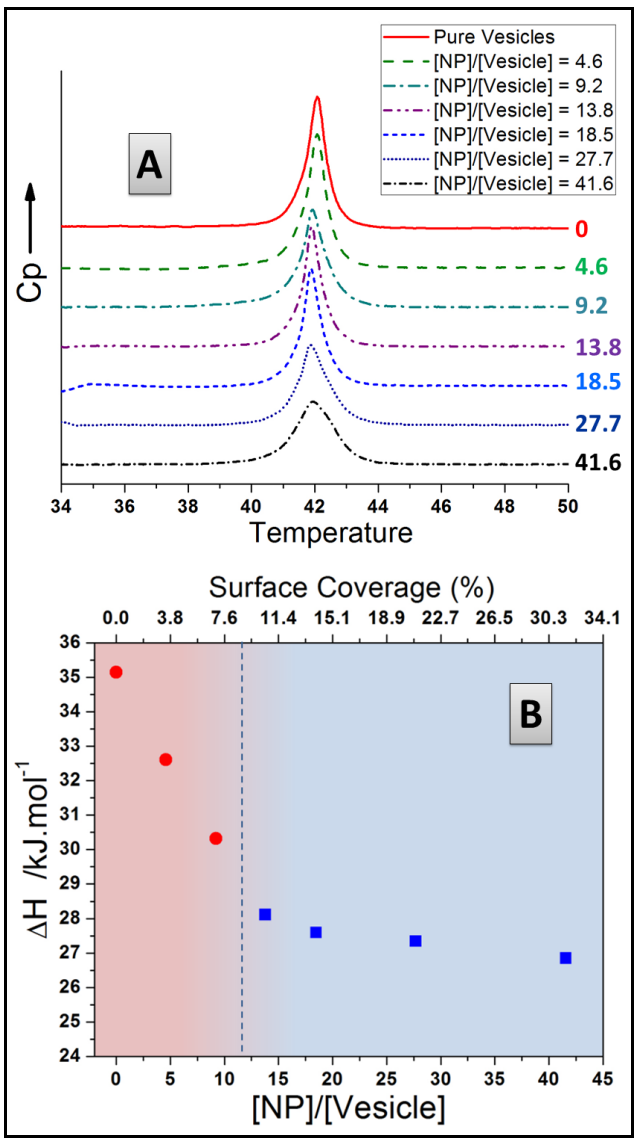


Fig.6: DSC thermograms (heating scans) of mixed SiNP/DPPC systems with increasing SiNP concentration featuring the main phase transition of the lipid membrane **(A)** and the corresponding transition enthalpies **(B).**

ζ-potential. The electric potential at the surface of colloids is related to the charge of the colloidal particles and their ability to repel each other. Therefore ζ-potential measurements give an insight into the stability of the colloidal system. Additionally, in our case, the ζ-potential gives an indication for the binding of the SiNPs on the surface of the liposomes and thus reveals the existence of decorated vesicle structures.

The potential values were obtained from the measured electrophoretic mobility on the basis of the Smoluchowski equation:

$$\mu_e = \frac{\varepsilon_r \varepsilon_0 \zeta}{\eta} \qquad (8)$$

where ε_r is the dielectric constant of the dispersion medium, ε_0 the permittivity of vacuum, η the dynamic viscosity of the medium, μ_e the electrophoretic mobility of the colloidal species, and ζ the ζ-potential. This equation is applicable in the case of large colloids with a "thin double layer" corresponding to the condition $\kappa R > 1$, where κ is the inverse of the Debye length. In this study, this condition is met in almost every case, as we are working with weakly charged and relatively large colloids (vesicles). Only for the pure nanoparticles at intermediate pH values, the product κR is around 1 since particles alone are small and strongly charged and the amount of NaOH and HCl added to adjust the pH at intermediate values is relatively low thereby leading to a slight underestimation of the potential values. The ζ-potentials of the different samples are presented in Figure 7 as a function of pH.

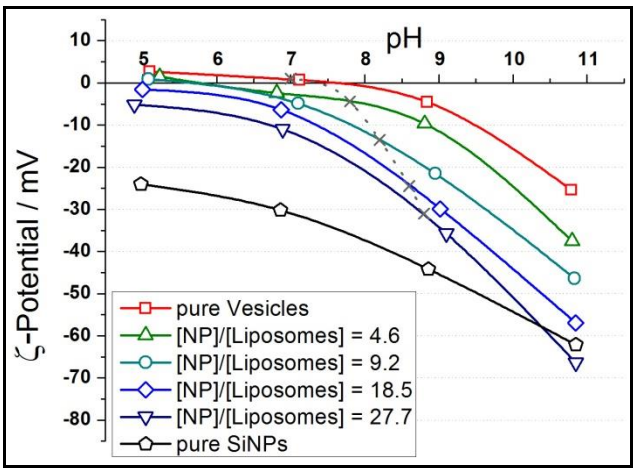


Fig. 7: ζ-Potential values at different pH of the pure vesicle solution, of the pure silica nanoparticle solution and of mixed systems SiNP/Liposome. The cross-shaped symbols linked by the dotted line represent the position of the samples used for visual inspection and DLS measurements, as mentioned above the pH was not controlled by a buffer in these samples as we worked at low ionic strength, thereby leading to data points which are not distributed vertically on this graph.

The pure DPPC solution has a ζ-potential around zero within experimental error at low and neutral pH and slightly negative at higher pH, consistent with the values expected for PC phospholipids, having an isoelectric point around pH = 4[41, 42] thereby being slightly negative at higher pH. Accordingly, the low surface potential is to be related with the instability of the pure vesicle system where the electrostatic repulsion between the weakly charged membranes is not sufficient to overcome the van der Waals interaction leading to vesicle encounters and subsequent fusion and/or agglomeration.

On the contrary, the ζ-potential of pure nanoparticles remains highly negative over the whole pH-range observed, revealing the highly charged nature of the silica nanoparticle surface in agreement with measurements made on different types of such silica particles.[23, 43]

In the case of the mixed systems, the addition of nanoparticles

to the liposome dispersions leads to progressively more negative values of the ζ-potential, which results from the charging of the vesicle surface and thereby confirms the mechanism of particle adsorption. If there would be no interaction between liposomes and SiNPs, it would be basically impossible to obtain one specific ζ-potential value for a given sample as we would obtain either two distributions of the electrophoretic mobility (one for the fast and highly charged particles and the other for the slower and weakly charged vesicles) or one distribution with a very high standard deviation (which is not the case here as shown by the small error bars on Figure 8).

Moreover, the observed decrease in surface potential is proportional to the amount of added particles, which is in agreement with assuming complete adsorption of the SiNPs on the vesicle surface. The addition of a low amount of nanoparticles leads to a slight decrease of the potential values which, at lower pH (5 to 9), are not negative enough to ensure sample stability (see results DLS/visual inspection). Accordingly, the addition of a larger amount of silica particles, above the limit represented by the ratio [NP]/[Vesicle] ~ 12 (see DLS), leads to more negative surface potential and subsequent improvement in sample stability due to sufficiently strong repulsive electrostatic interactions between the adsorbed particles.

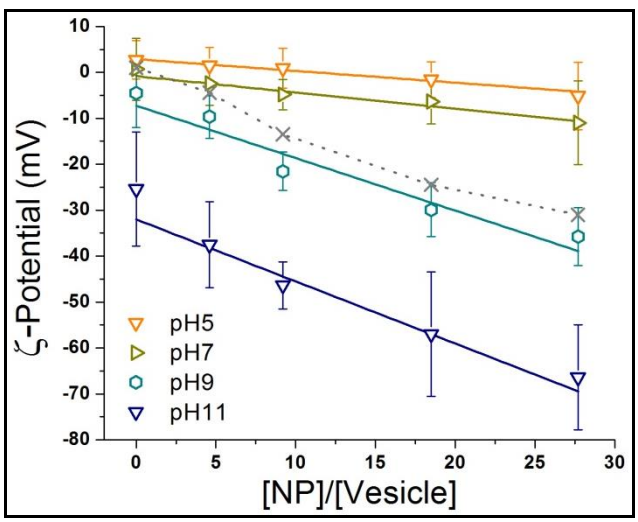


Fig. 8: ζ-Potential values of the mixed systems measured at different pH as a function of the calculated [NP]/[Vesicle] ratio (at 25 °C). The cross-shaped symbols linked by the dotted line represent the positions of the samples used for visual inspection and DLS measurements, as mentioned above the pH was not controlled for these samples leading to data points which are not exactly linearly distributed.

Dependence on pH and ionic strength. We also investigated the effects of pH and ionic strength on the stability behaviour of the hybrid SiNP/vesicle systems. For this purpose samples at controlled pH of 6 and 10 and one in PBS buffer (pH = 7.4) were prepared and followed by visual inspection and DLS as a function of time. The results are summarized in part d of the ESI (Figs. S5-S7).

These results show that samples at elevated pH 10 are similarly stable as the ones prepared without pH control, but in general showing a somewhat accelerated instability (Fig. S5 – ESI). Apparently the more negative ζ-potential (see Fig. 7) does not lead to a further stabilisation of the dispersed vesicles and also the critical amount of SiNPs required for having enhanced stability is not changed. An explanation for that behaviour could be that naturally the ionic strength at this pH is higher (around 5mM) and this effect then might be related to a correspondingly more pronounced screening of the electrostatic repulsion. An alternative explanation could be that at pH 10 the pure DPPC vesicles also have a pronouncedly negative ζ-potential of ~ 15 mV. The corresponding electrostatic repulsion to the SiNPs might lead to a lower tendency for adsorption of the particles on the vesicle surface and thereby to less stabilisation.

The samples at pH 6 are generally much less stable and here it is observed that addition SiNPs does not lead at all to an enhanced stability. In contrast, the samples are the more stable the less SiNPs they contain. This very pronounced effect should be related to the lower ζ-potential of the pure SiNPs at this pH (Fig. 7) but it is a bit surprising given the fact that the absolute value of the ζ-potential is not really so much smaller. Nonetheless at pH 6 the SiNPs effectively function as a precipitating agent for the vesicles and are not able to impart any stabilisation.

For the samples in PBS an even more pronounced instability upon addition of the SiNPs is observed. Here the addition of SiNPs to the vesicles leads in general to very rapid precipitation, irrespective of the amount of added SiNPs. This observation then has to be attributed to the much enhanced ionic strength for which the Debye screening length now is below 1 nm and apparently under such conditions the SiNPs are not able to lead to any electrostatic stabilisation of the SiNP/vesicle hybrid systems. Apparently the behaviour and, in particular, the stability conditions of the mixed SiNP/vesicle systems are very sensitive to pH and ionic strength. The most pronounced effects for the control of stabilisation are observed for low ionic strength and under neutral conditions.

Structure

ζ-potential. As mentioned above, the ζ-potential values become more negative with increasing nanoparticle concentration which is in good agreement with the formation of decorated vesicle structures in the bulk. Hence, the addition of more particles leads to the adsorption of more particles on the liposome surface thereby leading to the appearance of more charges on the decorated vesicle surface.

By plotting the measured ζ-potential as a function of the ratio [NP]/[Vesicle] (Fig. 8), one finds that the ζ-potential decreases linearly with the amount of particle in the solution. Taking into account the linear relation between surface charge and ζ-potential:

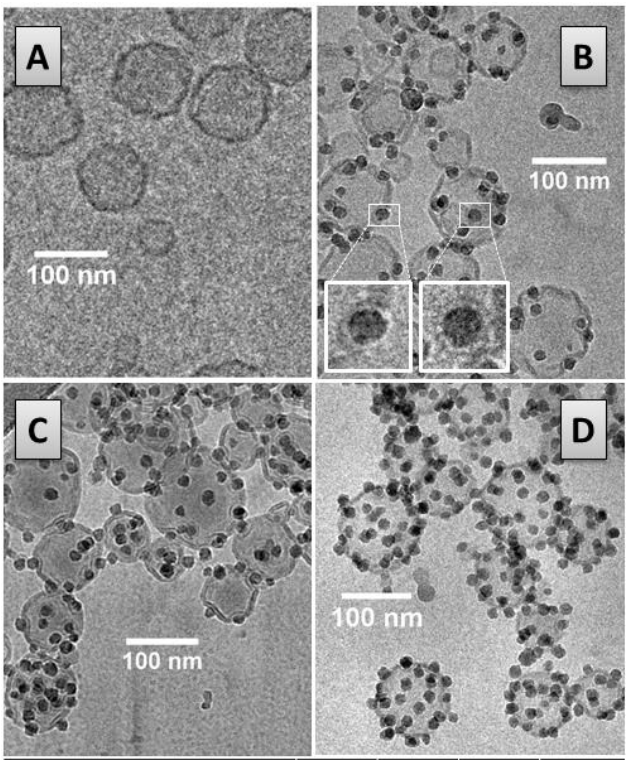
$$\zeta = \frac{1}{4\pi\varepsilon_r\varepsilon_0(1+\kappa R)}\frac{q}{R} \qquad (9)$$

where R is the radius of the colloidal species and q its charge, one can conclude that the number of nanoparticles adsorbed on each liposome increases linearly with the addition of particles in the solution in the concentration range investigated, in agreement with eq. 9.

Looking at this last result, the question of the systematic nature of the particle adsorption arises. In other words, one can make the assumption that every particle added to the system systematically adsorbs on a liposome, so that no particles remain free in the

solution.

Cryo-TEM. In order to gain further structural insights, cryo-TEM experiments on samples containing different amounts of added SiNPs and at constant concentration of 0.1wt% DPPC were done. In Fig. 9 some representative images for increasing SiNP concentrations are shown. As the sample temperature was well below the phase transition temperature one observes facetted unilamellar vesicles (Fig. 9A).



	A	B	C	D
[NP]/[Ves.] calc.	0	4.6	9.2	18.5
[NP]/[Ves.] CryoTEM	0	5.1	9.3	19.1

Fig. 9: Cryo-TEM Images of different mixed systems with increasing NP concentration. Comparison of the ratio of adsorbed NP per vesicle observed with cryo-TEM with the calculated [NP]/[Vesicle] values.

Upon increasing the concentration of added SiNPs one does not really observe a change of the vesicle size and morphology. However, the vesicles are now increasingly more decorated by the much smaller SiNPs, having rather low coverage in Fig. 9B and then being extensively covered in Fig. 9D. It can also be noted that apparently all added SiNPs are attached to the vesicles as no free SiNPs are observed in the electronmicrographs. It is important to note that the aggregated structures observed in these cryo-TEM images (especially 9B and 9C) cannot unquestionably be attributed to flocculation of the decorated vesicle structures as they may be due to a crowding effect at the edge of the grid holes where the thickness of the deposited film is higher than in the centre of the hole. However, the apparent trends for agglomeration seen in cryo-TEM parallel the experimental observations regarding colloidal stability.

The results from electron microscopy can also be analysed more quantitatively. The hypothesis of complete particle adsorption was confirmed using cryo-TEM and comparing the experimental number of nanoparticles found adsorbed per liposome in the TEM images with the ratio [NP]/[Vesicle] calculated from the sample composition (see bottom of Figure 9.). These two numbers are found very close to each other for all samples investigated ($0 < [NP]/[Vesicle] < 18.5$), thus confirming nicely that in this concentration range, basically all particles added to the solution are adsorbed on a liposome membrane and that the vesicle size is not affected by the interaction with the nanoparticles (as one could otherwise also have envisioned fusion process induced by the presence of the nanoparticles). However, in the case of the most concentrated sample ([NP]/[Vesicle] = 18.5) a few free nanoparticles are observed on some of the cryo-TEM images (see Fig. S3, ESI), but it should be noted that mostly we observed the situation as depicted in Fig. 9. Although their number is too low to dramatically influence the overall number of nanoparticles found adsorbed per liposome in the TEM images, their presence suggests the existence of a potential limit in the number of particles that can be adsorbed on one vesicle. This last result may be related to the slightly larger standard deviation on ζ-potential values obtained for the more concentrated mixed systems (see Fig. 8, for [NP]/[Vesicle] > 18), suggesting a higher polydispersity in size in agreement with the possible presence of free particles in the solution.

Further study of these cryo-TEM images leads to the observation of local membrane bending (see enlarged pictures Fig. 9.B) or indentations where the nanoparticles are adsorbed. This partial wrapping is due to the fact that the binding of the SiNPs occurred already at high temperature, when the phospholipid was in a fluid state and apparently this shape was retained during the cooling process. For such a binding to a fluid membrane, the shape and depth of this indentation depend on the balance between the attractive interaction between NP and membrane and the elastic energy required to bend the bilayer around the particle.[44, 45]

These local deformations have to be differentiated from the faceted structures observed on the pure liposomes (Fig.9.A), the latter being characteristic for gel phase membranes.[46]

It should be noted that in some rare cases for the systems in the unstable regime ([NP]/[vesicle] = 4.6 and 9.2) we also observed in the CryoTEM images the formation of some larger vesicles (Fig. S4, ESI). These might have been formed during the time when the membranes were still fluid, while for the later destabilisation we assume that that occurs primarily via agglomeration.

Discussion

The interaction between lipid bilayers and hydrophilic nanoparticles is rather complex and includes van der Waals, double layer, hydration, hydrophobic, thermal undulation and protrusion forces.[27]

In this study, we observed that the addition of negatively charged silica nanoparticles to a DPPC liposome solution leads to a systematic and complete adsorption of the particles onto the outer surface of the vesicles. This is the case as most of the forces contributing to the interaction silica/DPPC are attractive. Indeed, Van der Waals forces for similar systems have been found to be

attractive with a Hamaker constant in the range of (3-4)×10^{-21} J ≈ 0.75 to 1 *kT* (for *T* = 25°C).[47-49] Considering that an effective binding area of the NPs on the membrane will easily be that of a circle of 4 nm one ends up with binding energies in the range of 50 *kT* or more, which means that effectively this binding is irreversible. It is so large as the negative charges on the silica surface may interact with the positive charge of the lipid headgroups, this positive charge being known to be slightly closer to the surface for the case of DPPC.[24, 50] Furthermore the steric repulsion due to thermal fluctuations of the membrane is here suppressed as the DPPC bilayer is in a gel state at room temperature where undulations are reduced by the high rigidity of the membrane.

However, considering that the mixture is performed above the phase transition of the lipid, where the membrane is fluid,[51] a prolonged contact between particle and membrane would lead to an internalisation mechanism (or endocytosis)[44] rather than a simple particle adsorption. This has also been observed by us and will be the topic of a subsequent publication,[52] but from our experiments it was ascertained that for the short contact period at elevated temperature the process of internalisation could be neglected as it is occurring on a much longer time scale. Instead of internalisation, exclusively surface coverage takes place and once the sample is cooled down below the phase transition temperature, the decorated vesicles are frozen, leading to a substantial increase of their bending modulus,[51] and preventing further incorporation of particles.

Interestingly, the addition of nanoparticles to liposome dispersions and their adsorption onto the bilayer surface does not necessarily lead to vesicle stabilisation below their phase transition temperature. Below a certain concentration, the particles are found to accelerate liposomes agglomeration and thus promote their destabilisation.

This is the case as the quantity of adsorbed particles is not sufficient to ensure electrostatic repulsions between particles adsorbed on neighbouring liposomes. This has been reported in similar studies[25] and for the theoretical example of microspheres interacting with nanoparticles.[36] This effect is believed to be particularly strong in systems where there is significant size asymmetry, which is the case in the present system where the diameter of the charged silica particles is 5-6 times smaller than the vesicle diameter. Nevertheless, in these systems, it is quite challenging to define the precise mechanisms responsible for sample destabilisation and the structures it may result in. In general, once sediment is formed (in pure vesicle solutions as well as in the mixed systems) it could not be dispersed again by shaking the whole mixture. This would tend to reveal that coalescence is the phenomenon responsible for the destabilisation of the samples rather than flocculation. Nonetheless, the cryo-TEM images of these systems allow for the observation of only a few giant vesicles within SUV dispersions (Fig. S4 – ESI) so, that one is not able to conclude unequivocally on the processes responsible for the instability of the mixed systems.

Similarly, adding nanoparticles to vesicles in the gel state (instead of using a fluid phase vesicle dispersion, which is cooled down later, as performed in this study) leads to an instantaneous phase separation. This is probably due to the lower driving force of adhesion (the membrane cannot bend around the NPs) which will lead to a much slower decoration of the vesicles by NPs. Accordingly one will have for an extended period of time a situation of low coverage of the vesicles by NPs, which we have seen before (see Figs. 3 and 4) to be highly instable. This then leads to the destabilisation of these samples before they could be covered by a sufficiently large number of NPs to render them colloidally stable.

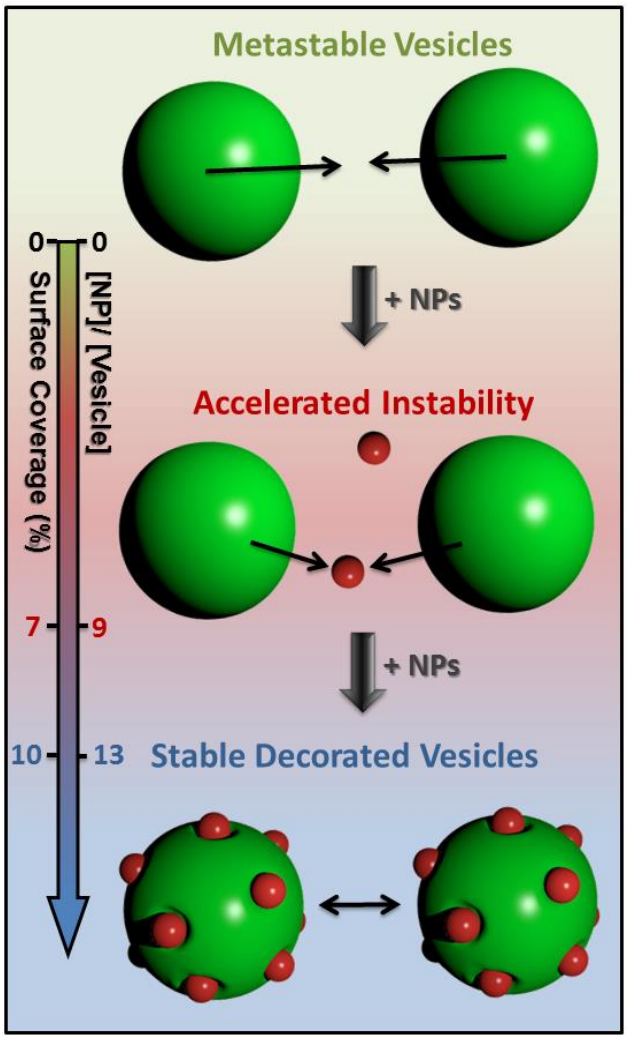


Fig. 10: Schematic drawing of the structural evolution and the stability of liposome dispersions upon addition of SiNPs.

However, coming back to the samples investigated in this study (prepared using the vesicle solution in its fluid phase and cooled down after the mixture with SiNPs), the addition of rather large amounts of particles ([NP]/[Vesicle] ≥ 12) leads to liposome stabilisation. This stabilisation effect is due to the adsorption of a sufficient amount of nanoparticles on the vesicle, thereby yielding vesicles with a coverage above 10% of the available surface. Apparently this coverage ensures the sufficient mutual repulsion between the adsorbed charged nanoparticles thereby preventing the encounter of neighbouring decorated liposomes thus slowing down the processes of coalescence or flocculation. Hence, a stable decorated vesicle dispersion is obtained. This is confirmed by the observation of potential values below -25 mV at pH above 7.5 (see Fig. 7 for samples having [NP]/[Vesicle] ≥ 12)

and the conservation of the mean hydrodynamic radius of the dispersions with time (see Fig. 4). Such a value of 25 mV for the ζ-potential has been found to be a typically required value for having colloidal stability,[53] but, of course, this is not a strict criterion for stability and for values higher or lower, the kinetics of destabilisation will be correspondingly slower or faster.

ζ-potential measurements are coherent with our analysis of these mixed systems. The ζ-potential values depend linearly on the ratio [NP]/[Vesicle] (see Fig. 8) and are confirmed by cryo-TEM as the observed average number of SiNPs adsorbed on one vesicle corresponds to the calculated ratio [NP]/[Vesicle]. This is important with respect to optimizing the amount of added nanoparticles to achieve liposome stabilisation.

Further analysis of the cryo-TEM images leads to a more detailed picture of the decorated vesicle structure. Due to the attractive interaction between membrane and particles already discussed above, there are indentations by the NPs into the membrane surface (see Fig. 9). The depth and size of these local deformations depend on the balance between the attractive energy and the bending energy required for this partial wrapping. However, we estimated before the attractive interaction to be well in the range of 50 *kT*, while the bending modulus of DPPC above the phase transition has been determined to be 9.5 *kT*,[51] which means that also the wrapping of the formerly rather flat membrane will only require about π times this value. This required energy for deformation is still less than the adhesive energy and this then explains the observed deformation of the membrane. In addition, this affects also its local stiffness as it induces local membrane deformations as evidenced by DSC (see Fig. 6), thereby leading to lower melting enthalpies. Moreover this will cause an additional interaction force between the different NPs adsorbed.

Conclusion

Comprehensive work on mixed liposome/nanoparticle systems has led to a detailed picture of the influence of the nanoparticle concentration on the stability of liposome dispersions, by the formation of nanoparticle-decorated vesicles. The stabilisation of such hybrid structures is achieved upon the systematic adsorption of a minimum amount of nanoparticles, below which particles bridge neighbouring liposomes, accelerating their aggregation in a systematic manner. The adsorption of a sufficient amount of particles leads to colloidal stabilisation of the decorated vesicle structures due to the introduction of sufficiently pronounced repulsive electrostatic forces whose strength increases linearly with increasing amount of nanoparticles. In our case of vesicles of 42 nm radius this stabilisation mechanism becomes fully active for mixed systems having a [NP]/[Vesicle] ratio larger than 12 (corresponding to a surface coverage above 10%).

These findings are not only of interest with respect to the fundamental interactions between nanoparticles and liposomes but also with respect to efficiently using small negatively charged silica nanoparticles (SiNPs) as stabiliser for pharmaceutical or cosmetic phospholipid dispersions, thereby aiding the formulation of such systems.

Acknowledgement

Financial support by the German Research Foundation (DFG) in the framework of the IGRTG 1524 (SSNI) is gratefully acknowledged. For instructive discussions we are grateful to T. Weikl. The support of the Russell-Berrie Nanotechnology Institute is acknowledged.

References

1. D. Marsh, *Chem. Phys. Lipids*, 1991, **57**, 109-120.
2. A. D. Bangham, M. M. Standish and J. C. Watkins, *J. Mol. Biol.*, 1965, **13**, 238-252.
3. M. Gradzielski, *J. Phys.-Condes. Matter*, 2003, **15**, R655-R697.
4. D. D. Lasic and D. Papahadjopoulos, *Medical applications of liposomes - Foreword*, Elsevier Science Bv, Amsterdam, 1998.
5. A. Sharma and U. S. Sharma, *Int. J. Pharm.*, 1997, **154**, 123-140.
6. G. Cevc, *Adv. Drug Deliv. Rev.*, 2004, **56**, 675-711.
7. A. Jesorka and O. Orwar, in *Annual Review of Analytical Chemistry*, Annual Reviews, Palo Alto, 2008, vol. 1, pp. 801-832.
8. D. D. Lasic, *Trends Biotechnol.*, 1998, **16**, 307-321.
9. R. M. Watwe and J. R. Bellare, *Curr. Sci.*, 1995, **68**, 715-724.
10. R. G. Laughlin, *Colloid Surf. A-Physicochem. Eng. Asp.*, 1997, **128**, 27-38.
11. E. Evans and M. Metcalfe, *Biophys. J.*, 1984, **46**, 423-426.
12. E. Evans and D. Needham, *J. Phys. Chem.*, 1987, **91**, 4219-4228.
13. R. Lipowsky, *Curr. Opin. Struct. Biol.*, 1995, **5**, 531-540.
14. N. Dos Santos, C. Allen, A. M. Doppen, M. Anantha, K. A. K. Cox, R. C. Gallagher, G. Karlsson, K. Edwards, G. Kenner, L. Samuels, M. S. Webb and M. B. Bally, *Biochim. Biophys. Acta-Biomembr.*, 2007, **1768**, 1367-1377.
15. A. Ishihara, M. Yamauchi, H. Kusano, Y. Mimura, M. Nakakura, M. Kamiya, A. Katagiri, M. Kawano, H. Nemoto, T. Suzawa and M. Yamasaki, *Int. J. Pharm.*, 2010, **391**, 237-243.
16. K. Kostarelos, T. F. Tadros and P. F. Luckham, *Langmuir*, 1999, **15**, 369-376.
17. D. D. Lasic, *Angew. Chem.-Int. Edit. Engl.*, 1994, **33**, 1685-1698.
18. S. Rangelov, K. Edwards, M. Almgren and G. Karlsson, *Langmuir*, 2003, **19**, 172-181.
19. M. C. Woodle and D. D. Lasic, *Biochimica Et Biophysica Acta*, 1992, **1113**, 171-199.
20. F. Quemeneur, M. Rinaudo, G. Maret and B. Pepin-Donat, *Soft Matter*, 2010, **6**, 4471-4481.
21. M. Rinaudo, F. Quemeneur and B. Pepin-Donat, *Int. J. Polym. Anal. Charact.*, 2012, **17**, 1-10.
22. M. M. Mady, M. M. Darwish, S. Khalil and W. M. Khalil, *Eur. Biophys. J. Biophys. Lett.*, 2009, **38**, 1127-1133.
23. S. Savarala, S. Ahmed, M. A. Ilies and S. L. Wunder, *ACS Nano*, 2011, **5**, 2619-2628.
24. Y. Yu, S. M. Anthony, L. F. Zhang, S. C. Bae and S. Granick, *J. Phys. Chem. C*, 2007, **111**, 8233-8236.
25. L. F. Zhang and S. Granick, *Nano Lett.*, 2006, **6**, 694-698.
26. G. Oberdorster, V. Stone and K. Donaldson, *Nanotoxicology*, 2007, **1**, 2-25.
27. R. Michel and M. Gradzielski, *Int. J. Mol. Sci.* , 2012, **13**, 11610-11642.
28. V. J. Mohanraj, T. J. Barnes and C. A. Prestidge, *Int. J. Pharm.*, 2010, **392**, 285-293.

29. P. Brocca, L. Cantu, M. Corti, E. Del Favero, S. Motta and M. C. Nodari, *Colloid Surf. A-Physicochem. Eng. Asp.*, 2006, **291**, 63-68.
30. M. Gugliotti, M. J. Politi and H. Chaimovich, *J. Colloid Interface Sci.*, 1998, **198**, 1-5.
31. M. J. Janiak, D. M. Small and G. G. Shipley, *Biochemistry*, 1976, **15**, 4575-4580.
32. D. Danino, *Curr. Opin. Colloid Interface Sci.*, 2012, **17**, 316-329.
33. D. Danino, A. Bernheim-Groswasser and Y. Talmon, *Colloid Surf. A-Physicochem. Eng. Asp.*, 2001, **183**, 113-122.
34. J. F. Nagle and S. Tristram-Nagle, *Biochim. Biophys. Acta-Rev. Biomembr.*, 2000, **1469**, 159-195.
35. P. S. Singh and V. K. Aswal, *J. Colloid Interface Sci.*, 2008, **326**, 176-185.
36. V. Tohver, J. E. Smay, A. Braem, P. V. Braun and J. A. Lewis, *Proc. Natl. Acad. Sci. U. S. A.*, 2001, **98**, 8950-8954.
37. B. J. Frisken, *Appl. Optics*, 2001, **40**, 4087-4091.
38. S. Ahmed and S. L. Wunder, *Langmuir*, 2009, **25**, 3682-3691.
39. S. Mabrey and J. M. Sturtevant, *Proc. Natl. Acad. Sci. U. S. A.*, 1976, **73**, 3862-3866.
40. B. Wang, L. F. Zhang, S. C. Bae and S. Granick, *Proc. Natl. Acad. Sci. U. S. A.*, 2008, **105**, 18171-18175.
41. A. D. Petelska and Z. A. Figaszewski, *Biophys. J.*, 2000, **78**, 812-817.
42. R. Zimmermann, D. Kuttner, L. Renner, M. Kaufmann, J. Zitzmann, M. Muller and C. Werner, *Biointerphases*, 2009, **4**, 1-6.
43. B. Bharti, J. Meissner and G. H. Findenegg, *Langmuir*, 2011, **27**, 9823-9833.
44. O. Le Bihan, P. Bonnafous, L. Marak, T. Bickel, S. Trepout, S. Mornet, F. De Haas, H. Talbot, J. C. Taveau and O. Lambert, *J. Struct. Biol.*, 2009, **168**, 419-425.
45. R. Lipowsky and H. G. Dobereiner, *Europhys. Lett.*, 1998, **43**, 219-225.
46. L. M. Ickenstein, M. C. Arfvidsson, D. Needham, L. D. Mayer and K. Edwards, *Biochim. Biophys. Acta-Biomembr.*, 2003, **1614**, 135-138.
47. T. H. Anderson, Y. J. Min, K. L. Weirich, H. B. Zeng, D. Fygenson and J. N. Israelachvili, *Langmuir*, 2009, **25**, 6997-7005.
48. P. S. Cremer and S. G. Boxer, *J. Phys. Chem. B*, 1999, **103**, 2554-2559.
49. J. Radler, H. Strey and E. Sackmann, *Langmuir*, 1995, **11**, 4539-4548.
50. B. Seantier and B. Kasemo, *Langmuir*, 2009, **25**, 5767-5772.
51. Z. Yi, M. Nagao and D. P. Bossev, *J. Phys.: Condens. Matter*, 2009, **21**, 155104.
52. R. Michel, T. Plostica, D. Danino and M. Gradzielski, *to be published*, 2013.
53. G. R. Wiese and T. W. Healy, *Transactions of the Faraday Society*, 1970, **66**, 490-499499.